Dimensionality efiects in vertical two-electron quantum dots in a perpendicular magnetic field

Journal of Physics: Conference Series **129** (2008) 012014 doi:10.1088/1742-6596/129/1/012014

Dimensionality effects in vertical two-electron quantum dots in a perpendicular magnetic field

R. G. Nazmitdinov [1,2] and N. S. Simonović [3]

[1] Departament de Física, Universitat de les Illes Balears, 07122 Palma de Mallorca, Spain
[2] BLTP, Joint Institute for Nuclear Research, 141980 Dubna, Russia
[3] Institute of Physics, P.O. Box 57, 11001 Belgrade, Serbia

E-mail: rashid@theor.jinr.ru

Abstract. The effect of third dimension on various physical properties of a two-electron vertical quantum dot is analysed. We show that at specific values the magnetic field gives rise to dynamical symmetries of the dot. A remarkable agreement between experimental data and calculations for the additional energy exhibits important role of the dot thickness for interpretation of ground state transitions in the magnetic field. We show that these transitions can be successfully reproduced as well in the two-dimensional approximation (only lateral confinement) but with the effective (screened) Coulomb interaction. We provide an analytical expression for the screening for the case of a parabolic vertical potential.

1. Introduction

Two-electron quantum dot (QD) is a benchmark system for experimental [1] and theoretical [2] studies of artificially trapped electrons in nanostructures. A competition between a confining potential, approximated quite well by the harmonic oscillator (HO), and repulsive electron-electron interaction produces a rich variety of phenomena in a perpendicular magnetic field. Being a simplest nontrivial system, QD He poses, however, a significant challenge to theorists.

Under the magnetic field one observes the angular momentum and spin oscillations of the ground state of the QDs with alteration of the field strength [1]. At certain field range the oscillations disappear and it is believed that the electrons form a finite-size analog of infinite integer quantum Hall liquid (with filling one) [2]. In QDs this fully polarized state is called the maximum density droplet (MDD). In recent single-electron spectroscopy measurements by Nishi *et al.* [3] it was found that the fully polarized triplet $(m, S) = (1, 1)$ state (MDD phase) can be replaced by the singlet $(2, 0)$ state in two-electron QDs at certain values of the magnetic field (m and S are the quantum numbers of the z-component of orbital momentum and the total spin, respectively). According to this reference, the ground state transition from the triplet $(1, 1)$ state to the singlet $(2, 0)$ state is associated with the collapse of MDD phase for $N = 2$. Using a two-dimensional (2D) He QD model, one is able to reproduce a general trend for the first singlet-triplet (ST) transitions observed in two-electron QDs under the magnetic field. However, the experimental positions of the first and next ST transition points are systematically higher [1, 3].

We recall thar a three-dimensional (3D) harmonic oscillator with frequencies in rational ratios (RHO) and a Coulomb system are benchmarks for the hidden symmetries which account for the

accidental degeneracies of their quantum spectra [4]. If the HO and the Coulomb potential are combined, like in the dot, most of the symmetries are expected to be broken. The classical dynamics of such a system is chaotic. The natural question arises is there any connection between classical dynamics and quantum properties of the system ?

The major aspect of the present communication is to demonstrate the importance of the QD thickness for various physical phenomena.

2. The Hamiltonian and hidden symmetries

The model Hamiltonian for the 3D two-electron QD reads

$$H=\sum_{i=1}^{2}\left\{\frac{1}{2m^*}(\mathbf{p}_i-\frac{e}{c}\mathbf{A}_i)^2+\frac{m^*}{2}\left[\omega_0^2(x_i^2+y_i^2)+\omega_z^2 z_i^2\right]\right\}+V_C+H_{\rm spin} \tag{1}$$

Here the term $V_C = k/|\mathbf{r}_1-\mathbf{r}_2|$ with $k = e^2/4\pi\epsilon_0\epsilon_r$ describes the Coulomb repulsion between electrons and $H_{\rm spin} = g^*\mu_B(\mathbf{s}_1+\mathbf{s}_2)\mathbf{B}$ is the Zeeman term, where $\mu_B = |e|\hbar/2m_e c$ is the Bohr magneton. For the perpendicular magnetic field we choose the vector potential with gauge $\mathbf{A}_i = \frac{1}{2}\mathbf{B}\times\mathbf{r}_i = \frac{1}{2}B(-y_i, x_i, 0)$. The confining potential is approximated with a 3D axially symmetric harmonic oscillator and $\hbar\omega_z \neq \hbar\omega_0$ are the energy scales of confinement in the z-direction and in the xy-plane, respectively. Here m^* and g^* are the effective electron mass and g-factor, respectively, and ε is the dielectric constant.

Introducing the relative and center-of-mass coordinates $\mathbf{r} = \mathbf{r}_1 - \mathbf{r}_2$, $\mathbf{R} = \frac{1}{2}(\mathbf{r}_1+\mathbf{r}_2)$, the Hamiltonian (1) can be separated into the center-of-mass (CM) $H_{\rm CM}$ and relative motion (RM) $H_{\rm rel}$ terms: $H = H_{\rm CM} + H_{\rm rel} + H_{\rm spin}$. The solution to the CM-Hamiltonian is well known [5] and the effect of the Zeeman energy has been discussed in [6, 7]. This term is not important for the dynamics of $H_{\rm rel}$ and will be taken into account only in numerical analysis of experimental data.

For our analysis it is convenient to use cylindrical *scaled* coordinates, $\tilde{\rho} = \rho/l_0$, $\tilde{p}_\rho = p_\rho l_0/\hbar$, $\tilde{z} = z/l_0$, $\tilde{p}_z = p_z l_0/\hbar$, where $l_0 = (\hbar/\mu\omega_0)^{1/2}$ is the characteristic length of the confinement potential with the reduced mass μ. For the sake of simplicity, we drop the tilde, i.e. for the scaled variables we use the same symbols as before scaling. The strength parameter k of the Coulomb repulsion goes over to $\lambda = k/(\hbar\omega_0 l_0)$. Typical for GaAs QDs values: $\hbar\omega_0 = 3\,$meV, $m^* = 0.067m_e$, dielectric constant $\varepsilon = 12$, – provide for the strength value $\lambda = 1.5$. In these variables the Hamiltonian for the relative motion takes the form (in units of $\hbar\omega_0$)

$$h \equiv \frac{H_{\rm rel}}{\hbar\omega_0} = h_0 + h_z + V_C = \frac{1}{2}\left(p_\rho^2 + \frac{m^2}{\rho^2} + {\omega_\rho}^2\rho^2 - \omega_L m\right) + \frac{1}{2}\left(p_z^2 + {\omega_z}^2 z^2\right) + \frac{\lambda}{r}, \tag{2}$$

where $r = (\rho^2+z^2)^{1/2}$, $m = l_z/\hbar$, $\omega_L = eB/2m^*c$ is the Larmor frequency and $\omega_\rho = (\omega_L^2+\omega_0^2)^{1/2}$ is the effective confinement frequency in the ρ-coordinate which depends through ω_L on the magnetic field and $\omega_{\rho,z,L} \Rightarrow \omega_{\rho,z,L}/\omega_0$. To find conditions, at which hidden symmetries can be manifested, we focus our analysis upon the nonlinear classical dynamics of the system.

Due to the cylindrical symmetry, the z-component $l_z \equiv p_\phi$ of the angular momentum is conserved and the motion in ϕ is separated from the motion in the (ρ, z)-plane. Since the Coulomb term couples the two coordinates, the problem is in general non-integrable which is reflected in the Poincaré sections shown in Fig. 1 for increasing magnetic field. There are, however, five integrable cases. The trivial cases are $\omega_z/\omega_\rho \to 0$ and $\omega_z/\omega_\rho \to \infty$, which correspond to 1D vertical and 2D circular QDs, respectively.

At the magnetic field $\omega_L'' = (\omega_z^2/4 - \omega_0^2)^{1/2}$ ($\omega_z/\omega_\rho = 2$) the motion becomes regular (see Fig.1b). In this case typical trajectories are exact parabolic arcs [8]. The use of the parabolic

coordinates (ξ, η, φ), where $\xi_1 = r + z$, $\xi_2 = r - z$, immediately leads to the separability of classical motion. In these coordinates the Hamiltonian (2) has the form

$$h = \frac{1}{\xi_1 + \xi_2}\left[2(\xi_1 p_{\xi_1}^2 + \xi_2 p_{\xi_2}^2) + \frac{m^2}{2}\left(\frac{1}{\xi_1} + \frac{1}{\xi_2}\right) + \frac{{\omega_z}^2}{8}(\xi_1^3 + \xi_2^3) + 2\lambda\right] - \omega_L'' m \tag{3}$$

and the equation $h(p_{\xi_1}, p_{\xi_2}, \xi_1, \xi_2) \equiv \epsilon$ is equivalent to the system

$$2\xi_j p_{\xi_j}^2 + \frac{m^2}{2\xi_j} + \frac{{\omega_z}^2}{8}\xi_j^3 - (\epsilon + \omega_L'' m)\xi_j + \lambda = (-1)^j c_z,\ j = 1, 2. \tag{4}$$

The separation constant $c_z = a_z - {\omega_\rho}^2 \rho^2 z$ appears as a third integral of motion. Here $a_z = (z p_\rho - \rho p_z) p_\rho + \left(\frac{m^2}{\rho^2} + \frac{\kappa}{r}\right) z$ is the z-component of the Laplace-Runge-Lenz vector $\mathbf{a} = \mathbf{p} \times \mathbf{l} + \kappa \mathbf{r}/r$ in (scaled) cylindrical coordinates. The vector $\mathbf{a}$ is a constant of motion for the pure Coulomb system (i.e. when $\omega_\rho = \omega_z = 0$) [4]. Note that for a two-electron QD the constant of motion c_z includes a space contribution as well.

At the value $\omega_L' = (\omega_z^2 - \omega_0^2)^{1/2}$ (see Fig.1d) the magnetic field gives rise to the spherical symmetry ($\omega_z/\omega_\rho = 1$) in an axially symmetric QD [9]. In this case the Hamiltonian (2) is separable in (scaled) spherical coordinates

$$h = \frac{p_r^2}{2} + \frac{(\mathbf{l}/\hbar)^2}{2r^2} + \frac{{\omega_z}^2 r^2}{2} + \frac{\lambda}{r} - \omega_L' m \tag{5}$$

and the dynamics is integrable. The additional integral of motion is the square of the total angular momentum $\mathbf{l}^2$.

At the magnetic field $\omega_L''' \equiv (4\omega_z^2 - \omega_0^2)^{1/2}$ (see Fig.1f) the Hamiltonian (2) is separable in the coordinates $\xi_1' = r + \rho$, $\xi_2' = r - \rho$ for $m = 0$. Note that for $m = 0$ the cases $\omega_z/\omega_\rho = 1/2$ and 2 are equivalent if we exchange the ρ and z coordinates and, hence, the additional integral of motion is $|a_\rho - {\omega_z}^2 z^2 \rho|$. However, for $m \neq 0$ the Hamiltonian (2) for $m \neq 0$ cannot be separated in these coordinates due to the term m^2/ρ^2. The separation for $m \neq 0$ is achieved by the virtue of the ansatz from Ref. [10]. It gives the desired integral of motion

$$C = [(a_\rho - {\omega_z}^2 z^2 \rho)^2 + a_\varphi^2 + 4m^2 {\omega_z}^2 r^2]^{1/2}. \tag{6}$$

Due to existence of three independent integrals of motion, h, m and C, which are in involution, the dynamics for $m \neq 0$, although non-separable, is integrable.

Although accurate numerical results for QD He can be obtained readily, the classical analysis provides the physical insight into numerical calculations. The results obtained with the aid of the Poincaré surfaces of sections are invariant under the coordinate transformation. On the other hand, the integrability is a necessary condition for the existence of a coordinate system in which the motion can be separated. In turn, the analogous quantum mechanical system would be characterized by a complete set of quantum numbers.

The Coulomb interaction destroys the general symmetry of the 3D HO. However, the magnetic field can recover symmetries which are common for the RHO and Coulomb systems. At a relatively low value of the magnetic field ω_L'' (for our parameters $B \approx 2.4\,\mathrm{T}$) we reveal the first manifestation of the hidden symmetries. This symmetry is determined by the integral of motion c_z. It results in the appearance of shells at each m-manifold [8]. There are exact crossings and repulsions between levels of different and of the same parity, respectively, in each shell. The near-degeneracy of the quantum spectrum is reminiscent of a striking degeneracy observed for the RHO or pure Coulomb systems. At higher values of the magnetic field ω_L' ($B \approx 7.5\,\mathrm{T}$), the dynamical spherical symmetry appears, since $\mathbf{l}^2$ becomes an additional integral

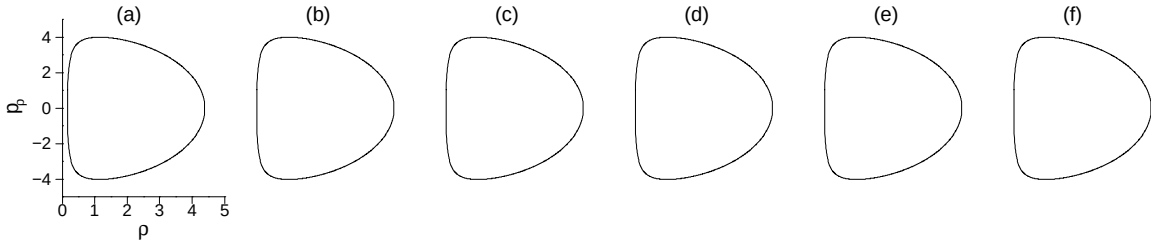

Figure 1. Poincaré surfaces of sections $z = 0$, $p_z > 0$ of the relative motion for the axially symmetric 3D two-electron quantum dot ($\lambda = 1.5$, $\epsilon = 10$, $m = 0$) with: (a) $\omega_z/\omega_\rho = 5/2$, (b) $\omega_z/\omega_\rho = 2$, (c) $\omega_z/\omega_\rho = 3/2$, (d) $\omega_z/\omega_\rho = 1$, (e) $\omega_z/\omega_\rho = 2/3$ and (f) $\omega_z/\omega_\rho = 1/2$. The sections (b), (d) and (f) indicate that for the corresponding ratios ω_z/ω_ρ the system is integrable.

of motion. This symmetry manifests itself as the attraction between levels with different orbital quantum numbers and the same parity. In contrast to spectra of pure Coulomb systems or of the RHO, there are no crossings between eigenstates of the subset characterized by a given quantum number m, since the accidental degeneracy is removed. Although the symmetry is recovered at very strong magnetic field ω_L''' ($B \approx 15.9\,\mathrm{T}$) due to the appearance of the integral of motion Eq. (6), the dynamics is non-separable for $m \neq 0$. Note that shells are similar to the spherical case.

The restoration of the rotational symmetry of the electronic states by the magnetic field for noninteracting electrons in 3D case was found within a simple shell model [11]. This phenomenon was also recognized in the results for *interacting* electrons in self-assembled QDs [12]. It was interpreted in [12] as an approximate symmetry that had survived from the noninteracting case due to dominance of the confinement energy over relatively small Coulomb interaction energy. However, as it is clear from the form of Eq.(5), the symmetry is *exact* even for strongly interacting electrons because the radial electron-electron repulsion does not break the rotational symmetry.

3. The collapse of MDD state in the two-electron QDs

As was discussed above, theoretical calculations [6, 7] assert that after the first ST transition the increase of the magnetic field induces several ground state transitions to higher orbital-angular and spin-angular momentum states. This issue was addressed in transport study of the correlated two-electron states up to 10 T in three vertical QDs [3]. In all samples clear shell structure effects for an electron number $N = 2, 6, ...$ at $B = 0$ T have been observed, implying a high rotational symmetry. Although there is a sufficiently small deviation from this symmetry in sample C (from now on in accordance with the list of Ref.[3]), a complete shell filling for two and six electrons was observed. Such a shell structure is generally associated with a 2D harmonic oscillator (x-y) confinement [1]. However, it is noteworthy that a similar shell structure is produced by a 3D axially symmetric HO if the confinement in the z-direction $\omega_z = 1.5\omega_0$ is only slightly larger than the lateral confinement ($\omega_x = \omega_y = \omega_0$). In this case six electrons fill the lowest two shells with Fock-Darwin energy levels with $n_z = 0$. It was also observed [3] that the lateral confinement frequency decreases with the increase of the electron number N. In turn, this effectively increases the ratio ω_z/ω_0 making the dot to be more "two-dimensional", since the vertical confinement is fixed by the sample thickness. All these facts imply that the 3D nature is a prerequisite of a consistent quantitative analysis of small QDs with a few electrons.

Our analysis is carried out by means of the exact diagonalization of the Hamiltonian (1). The evolution of the ground-state energy of a two-electron QD under the perpendicular magnetic field can be traced by means of the additional energy $\Delta\mu = \mu(2, B) - \mu(1, B)$, where

$\mu(N,B) = E(N,B) - E(N-1,B)$ and $E(N,B)$ denotes the total energy of the QD with N electrons under a magnetic field of the strength B [1]. Fitting the B-field dependence of the first and second Coulomb oscillation peak positions to the lowest Fock-Darwin energy levels of the 2D HO with the potential $m^*\omega_0^2 r^2/2$, Nishi *et al.* [3] estimated ω_0 for all three samples A, B, C. Although the general trend in the experimental data is well reproduced by the 2D calculations, the experimental positions of the ST transition points are systematically higher (see Fig.3 of Ref.[3]). Different lateral confinements in the above experiment are achieved by the variation of the electron density, without changing the sample thickness. Using the "experimental" values for the lateral confinement and the confinement frequency ω_z as a free parameter, we found [13] that the value $\hbar\omega_z = 8$ meV provides the best fit for the positions of kinks in the additional energy

$$\Delta\mu = \hbar\omega_0\varepsilon - E(1,B) + E_Z \tag{7}$$

in all three samples [13]. Here $\hbar\omega_0\varepsilon$ is the relative energy, $E(1,B) = \hbar\omega_0 + \hbar\omega_z/2$ and $E_Z = g^*\mu_B B[1-(-1)^m]/2$ is zero for the singlet states $m = 0, 2, ...$ It was found from the Zeeman splitting at high magnetic fields that $|g^*| = 0.3$ [14] and we calculated the additional energy with this and the bulk ($|g^*| = 0.44$) values.

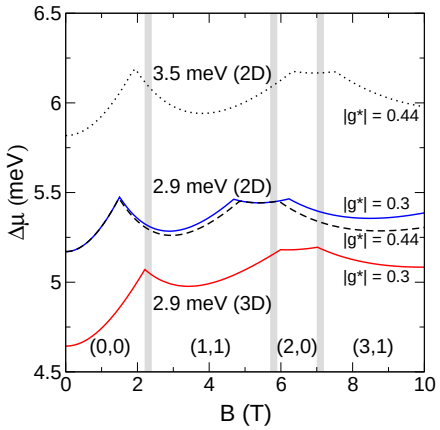

Figure 2. The addition energy $\Delta\mu$ as a function of the magnetic field for the 2D model with $\hbar\omega_0 = 2.9, 3.5$ meV and for the 3D model ($\hbar\omega_0 = 2.9$ meV, $\hbar\omega_z = 8$ meV). Ground states are labeled by (m,S) (see text). Grey vertical lines indicate the position of the experimental crossings between different ground states. From Ref.[13]

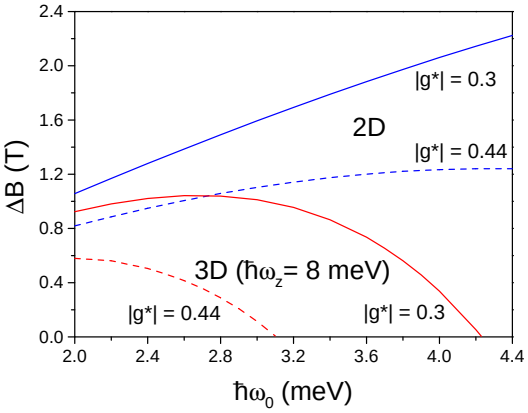

Figure 3. The interval ΔB in which the singlet state $(2,0)$ survives as a function of the lateral confinement for 2D and 3D calculations. The confinement in the third (z) direction $\hbar\omega_z = 8$ meV is fixed for the 3D calculations. From Ref.[13].

The most complete experimental information is related to sample C and let us study this sample in detail. In sample C the first experimental ST transition occurs at $B = 2.3$ T, while the signatures of the second and the third ones are observed at $B \approx 5.8, 7.1$ T, respectively (see Fig.2). The 2D calculations (with the "experimental" values $\hbar\omega_0 = 2.9$ meV, $|g^*| = 0.44$) predict the first, second and third ST crossings at lower magnetic fields: $B = 1.7, 4.8, 5.8$ T, respectively (see Fig.2). The results can be improved to some degree with $|g^*| = 0.3$. To reproduce the data for $\Delta\mu$ Nishi *et al.* [3] have increased the lateral confinement ($\hbar\omega_0 = 3.5$ meV, $|g^*| = 0.44$). As a result, the first, second and third ST transitions occur at $B = 2, 6.3, 7.5$ T, respectively.

Evidently, 2D calculations overestimate the importance of the Coulomb interaction. The increase of the lateral confinement weakens simply the electron correlations in such calculations. In contrast, the 3D calculations reproduce quite well the positions of all crossings with the "experimental" lateral confinement $\hbar\omega_0 = 2.9$ meV at $B = 2.3, 5.8, 7.1$ T (see Fig.2).

One of the questions addressed in the experiment [3] is related to a shoulderlike structure observed in a small range of values of the magnetic field (see Fig.4 of [3]). This structure is identified as the second singlet state $(2,0)$ that persists till the next crossing with the triplet state $(3,1)$. According to Ref.[3], the ground state transition from the triplet $(1,1)$ state to the singlet $(2,0)$ is associated with the collapse of MDD state for $N = 2$. Therefore, a question arises: at which conditions it would be possible to avoid the collapse of the MDD phase (in general, to preserve the spin-polarized state); i.e., at which conditions the singlet $(2,0)$ state never will show up in the ground state. In fact, the collapse of the MDD depends *crucially* on the value of the lateral confinement and *the dimension* of the system. We found that in the 2D consideration the $(2,0)$ state always exists for experimentally available lateral confinement (see Fig.3). Moreover, in this range of ω_0 the 2D approach predicts the monotonic increase of the interval of values of the magnetic field ΔB, at which the second singlet state survives, with the increase of the lateral confinement. In contrast, in the 3D calculations, the size of the interval is a vanishing function of the lateral confinement for a fixed thickness ($\hbar\omega_z = 8$ meV). It is quite desirable, however, to measure this interval to draw a definite conclusion and we hope it will done in future.

4. Effective charge

In real samples the confining potential in the z-direction is much stronger than in the xy-plane. This fact is, usually, used to justify a 2D approach for study of QDs. However, there is a nonzero contribution from the vertical dynamics, since the energy level available for each of noninteracting electrons in z-direction is $\varepsilon = \hbar\omega_z(n_z + 1/2)$. For the lowest state $n_z = 0 \Rightarrow \varepsilon_1 = \frac{1}{2}\hbar\omega_z$. By dint of the condition $V_z(\pm z_m) \equiv m^*\omega_z^2 z_m^2/2 = \varepsilon_1$ one defines the turning points: $z_m = \sqrt{\hbar/(m^*\omega_z)}$. We assume that the distance between turning points should

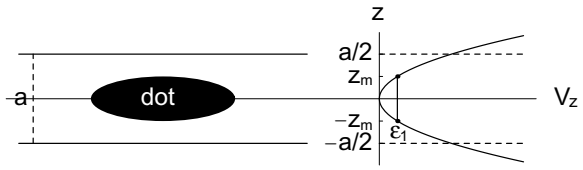

Figure 4. Left: the localization of QD in the layer of the thickness a. Right: the schematic representation of the position of zero-point motion in the parabolic confinement relative to the layer thickness.

not exceed the layer thickness, i.e. $2z_m \leq a$ (see Fig.4). In virtue of this inequality it follows that the lowest limit for the vertical confinement in the layer of thickness a is $\hbar\omega_z \geq 4\hbar^2/(m^*a^2)$. For typical GaAs samples with the thickness a between 10 nm and 20 nm this estimation gives the minimal value for $\hbar\omega_z$ between 45 meV and 11 meV, respectively. It results in different time scales, i.e., $T_z(= 2\pi/\omega_z) \ll T_0(= 2\pi/\omega_0)$ and this allows one to use the adiabatic approach [15].

To lowest order the adiabatic approach consists of averaging the 3D Hamiltonian (1) over the angle-variables $\theta_{z_i} = \omega_{z_i}t$ (fast variables) of the unperturbed motion ($k = 0$) of two electrons after rewriting the (z_i, p_{z_i}) variables in terms of the action-angle variables (J_{z_i}, θ_{z_i}) (see details in Appendix A in [9]). As a result, one obtains the effective electron-electron interaction (see Appendix B in [9])

$$V_{\rm int}^{\rm eff}(\rho; J_z) = \frac{2k}{\pi\rho}\, K\!\left(-\frac{2J_z}{\mu\omega_z\rho^2}\right), \tag{8}$$

where $K(x)$ is the complete elliptic integral of the first kind. The effective Hamiltonian for the relative motion is $H_{\rm rel}^{\rm eff} = h_0 + V_{\rm int}^{\rm eff}(\rho; J_z) + E_z^{\rm rel}$, where $E_z^{\rm rel} = \omega_z J_z = \hbar\omega_z(n_z + 1/2)$.

Our *ansatz* consists in the consideration of the effective interaction (8) in the form $V_{\rm int}^{\rm eff} = kf(\rho)/\rho$. Then one can define the effective 2D Coulomb interaction $V_C^{\rm eff} = k_{\rm eff}/\rho$, where the effective charge is the mean value of the factor $f(\rho)$ upon the nonperturbed lateral wave functions (Fock-Darwin states), i.e., $k_{\rm eff} = k\langle f(\rho)\rangle \equiv \langle \rho\, V_{\rm int}^{\rm eff}(\rho)\rangle = 2k\left\langle n_\rho, m\middle| K\left(-\frac{\hbar\,(2n_z+1)}{\mu\omega_z\rho^2}\right)\middle| n_\rho, m\right\rangle/\pi$. For the lowest states ($n_\rho = n_z = 0$) the effective charge is expressed in terms of the Meijer G-function [16]

$$k_{\rm eff} = \frac{k}{\pi|m|!}\, G_{2,3}^{2,2}\left(\frac{\omega_\rho}{\omega_z}\middle|\begin{array}{ccc} 1/2 & 1/2 \\ 0 & m+1 & 0 \end{array}\right). \tag{9}$$

Guided by the adiabatic approach, it is instructive to compute the effective charge by dint of quantum-mechanical mean value of the Coulomb term in the 3D oscillator state $|n_\rho, m\rangle|n_z\rangle$: $k_{\rm eff} = \langle\langle \rho\, V_C(\rho, z)\rangle\rangle = k\,\langle\langle (1 + z^2/\rho^2)^{-1/2}\rangle\rangle$. Here, $|n_z\rangle$ is a normalized one-dimensional harmonic oscillator wave function [4]. Since the lateral extension exceeds the thickness of the QDs by several times, one may suggest to consider the ratio $(z/\rho)^2$ as a small parameter of theory. Note, however, that the averaging over the 3D oscillator state $|n_\rho, m\rangle|n_z\rangle$ implies the application of the first order perturbation theory for calculation of the contribution of the Coulomb interaction in QDs. For $n_\rho = n_z = 0$ one obtains

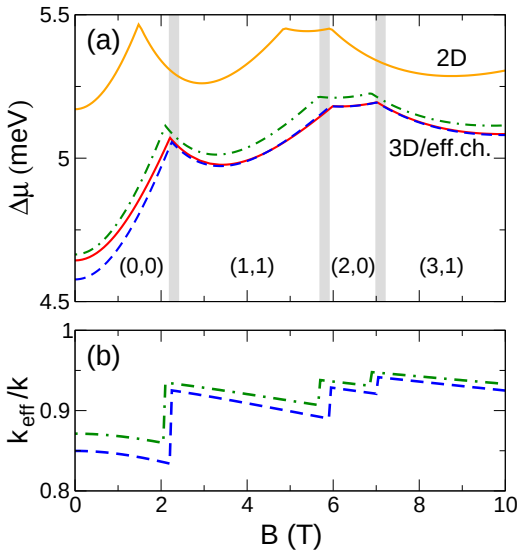

Figure 5. (a)Similar to Fig.2. The results of plain 2D calculations ($\hbar\omega_0 = 2.9\,$meV, $|g^*| = 0.3$) and full 3D approach [13] ($\hbar\omega_z = 8\,$meV) are connected by solid lines, respectively. The vertical grey lines indicate the position of the experimental crossings between different ground states in a sample C [3]. The results based upon the adiabatic approximation, Eq.(9), and the plain quantum-mechanical averaging procedure, Eq.(10), are connected by dashed and dot-dashed lines, respectively. (b) The ratio $k_{\rm eff}/k$ as functions of the magnetic field based on Eq.(9) and the plain quantum-mechanical averaging, Eq.(10) are connected by dashed and dot-dashed lines, respectively.

$$k_{\rm eff} = k\frac{2}{|m|!}\left(\frac{\mu\omega_\rho}{\hbar}\right)^{|m|+1}\sqrt{\frac{\mu\omega_z}{\pi\hbar}}\int_0^\infty K_0\left(\frac{\mu\omega_z\rho^2}{2\hbar}\right) e^{\mu(\frac{1}{2}\omega_z-\omega_\rho)\rho^2/\hbar}\rho^{2|m|+2}\,d\rho, \tag{10}$$

where K_0 is the modified Bessel function of the 2nd kind. One observes that in both definitions of the effective charge Eqs.(9),(10) there is a contribution of the electron dynamics along the coordinate z.

The results of calculations (see Fig.5) of the additional energy in 2D approximation (with the effective Coulomb interaction) and in 3D approach with a full Coulomb interaction demonstrate the remarkable accord between the predictions based on the effective charge approach and the

observation. Note that the results based upon the adiabatic approximation are in a better agreement with the full 3D calculations in contrast to those obtained with the aid of the plain quantum-mechanical averaging procedure for $k_{\rm eff} = \langle\langle \rho\, V_C(\rho, z)\rangle\rangle$. As discussed above, the adiabatic approach is based on the effective separation of fast (vertical) and slow (lateral) dynamics with subsequent averaging procedure. In contrast, the plain quantum-mechanical averaging represents a type of perturbation theory based upon the first order contribution with respect to the ratio z/ρ only. The increase of the quantum number m, caused by the increase of the magnetic field strength, reduces the orbital motion of electrons in the vertical direction. The larger is m the stronger is the centrifugal forces, which induce the electron localization in a plane, and, therefore, the lesser is importance of the vertical electron dynamics. In the limit of strong magetic field (large m) the dot becomes more a "two-dimensional" system. This explains the improvement of the accuracy of the plain quantum-mechanical averaging procedures at large m, i.e., for the ground states at high magnetic fields.

5. Summary

We demonstrated that the confinement in the z direction is important ingredient for the quantitative analysis of the experimental data for two-electron axially symmetric vertical QDs. Quantum spectra of such QDs exhibit hidden symmetries at certain values of the magnetic field. This fact has been overlooked in a plain quantum-mechanical models. The onset of the symmetries, for example, at ω_L'' leads to a singlet-triplet degeneracy which should increase the conductance at this value of the magnetic field. We developed the effective charge approach taking full account of the thickness of two-electron QDs. Using the adiabatic approximation, based on action-angle variables, we have derived the analytical expression for the screening which facilitates the numerical calculations.

Acknowledgments

This work was partly supported by Project No 141029 of Ministry of Science and Environmental Protection of Serbia, Grant No. FIS2005-02796 (MEC, Spain) and Grant of RFBR 08-02-00118 (Russia).

[1] Kouwenhoven L P, Austing D G, and Tarucha S 2001 *Rep. Prog. Phys.* **64** 701
[2] Reimann S M and Manninen M 2002 *Rev. Mod. Phys.* **74** 1283
[3] Nishi Y, Tokura Y, Gupta J, Austing G and Tarucha S 2007 *Phys. Rev. B* **75** 121301(R)
[4] Landau L D and Lifshitz E M 1977 *Quantum Mechanics* (Oxford: Pergamon Press)
[5] Fock V 1928 *Z. Phys.* **47** 446; Darwin C G 1930 *Proc. Cambridge Philos. Soc.* **27** 86
[6] Merkt U, Huser J and Wagner M 1991 *Phys.Rev.B* **43** 7320; Wagner M, Merkt U and Chaplik A V 1992 *Phys. Rev.B* **45** 1951
[7] Dineykhan M and Nazmitdinov R G 1997 *Phys. Rev.B* **55** 13707; 1999 *J. Phys.: Condens.Matter* **11** L83
[8] Simonović N S and Nazmitdinov R G 2003 *Phys. Rev. B* **67** 041305(R)
[9] Nazmitdinov R G, Simonović N S, and Rost J.-M 2002 *Phys. Rev. B* **65** 155307
[10] Blümel R, Kappler C, Quint W and Walther H 1989 *Phys. Rev. A* **40** 808
[11] Madhav A V and Chakraborty T 1994 *Phys. Rev. B* **49** 8163; Heiss W D and Nazmitdinov R G 1998 *Pis'ma v ZhETF* **68** 870 (*JETP Lett.* **68** 915)
[12] Wojs A, Hawrylak P, Fafard S, and Jacak L 1996 *Phys. Rev. B* **54** 5604
[13] Nazmitdinov R G and Simonović N S 2007 *Phys. Rev. B* **76** 193306
[14] Nishi Y, *et al.* 2006 *Phys. Rev. B* **74** 033306
[15] Lichtenberg A J and Liberman M A 1983 *Regular and Stochastic Motion* (New York: Springer)
[16] Gradshteyn I S and Ryzhik I M 1994 *Table of Integrals, Series, and Products* Fifth Edition (New York: Academic Press) pp 898,1096